

POWER FLOW IN A PLATE WITH AN ATTACHED POINT DAMPER

Sabih I. Hayek *, Moongyung Nam *, and Scott D. Sommerfeldt #

*Department of Engineering Science and Mechanics, # Graduate Program in Acoustics, Penn State University, University Park, PA, 16802

INTRODUCTION

Mechanical power due to flexural vibration flows from mechanical sources which can be transmitted through a structure, such as an elastic plate, to another attached structure that is connected to the first at a single point. The connected structure can dissipate this energy through coupling to an acoustic medium or transmit it to yet a third structure. The objective of this work is to investigate the path of power flow from a mechanical source to any point in a plate by plotting the vector structural intensity (SI) map. A damped, simply supported plate is taken as a model for the support structure and a point damper (PD), whose resistive point impedance acts as an energy absorbing device, and models the power flow transmission to a connected structure. The damping coefficient of the PD represents a measure of the power flow through the connection point. The analysis and measurement of Structural Intensity (SI) has been studied by few authors, which was the subject of two congresses [1]. The measurement of SI has been reported in Ref[2-7].

STRUCTURAL INTENSITY OF A PLATE

The SI vector is the mechanical power flow per vector unit area, which has direction and magnitude as a function of position in the structure. Thus, a structural intensity map shows the power flow from a mechanical source to any point in the plate. The real part of the structural intensity is known as the active intensity and propagates along the structure representing the net power flow. The x- and y- components of the instantaneous structural intensity vector of an elastic plate obeying the classical Bernoulli-Euler theory can be expressed as :

$$\begin{aligned}
 I_x(x, y, t) &= - \left(V_x \frac{\partial W}{\partial t} + M_x \frac{\partial \Theta_x}{\partial t} + M_{yx} \frac{\partial \Theta_y}{\partial t} \right) \\
 I_y(x, y, t) &= - \left(V_y \frac{\partial W}{\partial t} + M_y \frac{\partial \Theta_y}{\partial t} + M_{yx} \frac{\partial \Theta_x}{\partial t} \right)
 \end{aligned}
 \tag{1}$$

The first term of eq. (1) is the product of the shear force and the transverse velocity. The second term is the product of the bending moment and the associated angular velocity. The third term is the product of the twisting moment and the associated angular velocity. The bending moments (M_x, M_y), the twisting moment M_{yx} , the transverse shear forces (V_x, V_y) and the rotational displacements (Θ_x, Θ_y) can be expressed in terms of the spatial derivatives of the transverse displacement $W(x, y, t)$. With conventional sign notation, these are given by :

$$\begin{aligned}
 M_x &= -D \left(\frac{\partial^2 W}{\partial x^2} + \nu \frac{\partial^2 W}{\partial y^2} \right) & M_y &= -D \left(\frac{\partial^2 W}{\partial y^2} + \nu \frac{\partial^2 W}{\partial x^2} \right) \\
 V_x &= -D \frac{\partial}{\partial x} \left(\frac{\partial^2 W}{\partial x^2} + \frac{\partial^2 W}{\partial y^2} \right) & V_y &= -D \frac{\partial}{\partial y} \left(\frac{\partial^2 W}{\partial x^2} + \frac{\partial^2 W}{\partial y^2} \right) \\
 M_{xy} &= M_{yx} = -D(1-\nu) \left(\frac{\partial^2 W}{\partial x \partial y} \right) \\
 \Theta_x &= -\frac{\partial W}{\partial x} & \Theta_y &= -\frac{\partial W}{\partial y}
 \end{aligned} \tag{2}$$

Here D is the bending rigidity, given by $D = Eh^3/12(1-\nu^2)$, where ν is Poisson's ratio, E is the Young's modulus of the material, and h is the plate thickness. Inserting eq. (2) into eq. (1), one can express the structural intensity components for a thin plate in terms of the transverse displacement $W(x, y, t)$. If complex quantities are used to represent a field with simple harmonic time dependence, the time-averaged complex structural intensity, $\tilde{\tilde{I}}$, can be defined as:

$$\begin{aligned}
 \tilde{\tilde{I}}(x, y) &= \tilde{I}_x(x, y) \bar{e}_x + \tilde{I}_y(x, y) \bar{e}_y \\
 &= (\tilde{I}_x(x, y) + j\tilde{Q}_x(x, y)) \bar{e}_x + (\tilde{I}_y(x, y) + j\tilde{Q}_y(x, y)) \bar{e}_y,
 \end{aligned} \tag{3}$$

where the x- and y-components are expressed by

$$\begin{aligned}
 \tilde{I}_x(x, y) &= \frac{1}{2} j\omega \left\{ \tilde{V}_x(x, y) \tilde{W}^*(x, y) + \tilde{M}_x(x, y) \tilde{\Theta}_x^*(x, y) + \tilde{M}_{xy}(x, y) \tilde{\Theta}_y^*(x, y) \right\} \\
 \tilde{I}_y(x, y) &= \frac{1}{2} j\omega \left\{ \tilde{V}_y(x, y) \tilde{W}^*(x, y) + \tilde{M}_y(x, y) \tilde{\Theta}_y^*(x, y) + \tilde{M}_{xy}(x, y) \tilde{\Theta}_x^*(x, y) \right\}
 \end{aligned} \tag{4}$$

Here, the bar (-) denotes the time-averaged values, the tilde (~) denotes complex quantities and the asterisk (*) denotes the complex conjugate. The active and reactive intensity vectors in a thin plate can now be expressed as follows by taking the real and imaginary parts, respectively:

$$\begin{aligned}
 \tilde{I}(x, y) &= \tilde{I}_x(x, y) \bar{e}_x + \tilde{I}_y(x, y) \bar{e}_y \\
 \tilde{Q}(x, y) &= \tilde{Q}_x(x, y) \bar{e}_x + \tilde{Q}_y(x, y) \bar{e}_y,
 \end{aligned} \tag{5}$$

Response of a Simply Supported Plate Excited by a Point Force and Connected to a Point Damper. Consider a thin elastic rectangular plate to which a PD with a damping coefficient C is attached at the position (x_d, y_d) and a harmonic point force is located at (x_o, y_o) . The plate is simply supported with dimensions $L_x \times L_y$, thickness h , and mass density ρ . The governing equation of motion for the transverse displacement $W(x, y, t)$ is expressed as :

$$\tilde{D} \nabla^4 W + \rho h \frac{\partial^2 W}{\partial t^2} + C \frac{\partial W}{\partial t} \delta(x - x_d) \delta(y - y_d) = F_o \delta(x - x_o) \delta(y - y_o) \cos(\omega t - \phi) \tag{6}$$

where ω is the angular frequency of the applied force. F_o is the amplitude of a simple harmonic point force applied at location (x_o, y_o) . \tilde{D} , given by $\tilde{D} = D(1 + j\eta)$, is the complex dynamic bending rigidity which includes internal structural damping, whose damping coefficient is η .

Substituting the displacement $W(x, y, t)$, into eq. (6) and introducing the wave number k , defined from $\rho h \omega^2 / D = k^4$, the PD's damping factor β , defined from $C^2 / \rho h D = \beta^4$, and the point force, represented with a complex amplitude $\tilde{F}_o = F_o e^{-i\theta}$, results in :

$$\tilde{D} \nabla^4 \tilde{W} - D k^4 \tilde{W} + j D (\beta k)^2 \tilde{W} \delta(x - x_d) \delta(y - y_d) = \tilde{F}_o \delta(x - x_o) \delta(y - y_o) \quad (7)$$

The response of a damped system can be expressed in terms of a series of eigenfunctions of the undamped system. Thus, the complex transverse displacement $\tilde{W}(x, y)$ may be expressed as

$$\tilde{W}(x, y, \omega) = \sum_{m=1}^{\infty} \sum_{n=1}^{\infty} \tilde{B}_{mn}(\omega) W_{mn}(x, y) \quad (8)$$

where $W_{mn}(x, y) = \sin k_m x \sin k_n y$ is the modal shape function for the m, n mode of a simply supported undamped plate. $k_m = m\pi/L_x$ and $k_n = n\pi/L_y$ are the modal wave numbers, while m and n are the modal indices in the x and y directions, respectively. $\tilde{B}_{mn}(\omega)$ is the complex modal amplitude coefficient to be determined. Substituting the solution in eq. (8) in eq.(7), and using the orthogonality of the eigenfunctions, one obtains:

$$DN(\tilde{k}_{mn}^4 - k^4) \tilde{B}_{mn} + jD(\beta k)^2 \{W_{mn}^2(x_d, y_d) \tilde{B}_{mn} + \sum_{\substack{p=1 \\ p \neq m}}^{\infty} \sum_{\substack{q=1 \\ q \neq n}}^{\infty} W_{mn}(x_d, y_d) W_{pq}(x_d, y_d) \tilde{B}_{pq}\} = \tilde{F}_o W_{mn}(x_o, y_o) \quad (9)$$

where the complex modal wave number \tilde{k}_{mn} is obtained from $\tilde{k}_{mn}^4 = k_{mn}^4 (1 + j\eta)$, $k_{mn} = ((m\pi/L_x)^2 + (n\pi/L_y)^2)^{1/2}$. The modal amplitudes $\tilde{B}_{mn}(\omega)$ can be obtained by solving a subset of the infinite set of algebraic linear equations in eq. (9). For this study a 225x225 matrix of equations were solved to cover modes up to $m=15$, and $n=15$.

NUMERICAL RESULTS

Consider a steel plate that has the dimensions 0.60x0.40x0.0032 m., density 7800 Kg/m³, and Young's modulus of 2.06x10¹¹ N/m². A 1N point force is located at (0.15, 0.15m), and a point damper is located at (0.50, 0.10m). To investigate the influence of the structural damping on the power flow of an internally damped plate, the SI is computed for a range of values of $\eta = 0, 0.01, 0.1$, and $C=0, 5, 20, 50, 100$, and 200 Nsec/m. The excitation was taken as either at the resonance frequency of 280 Hz., representing the (2,2) mode, or at the off-resonance frequency of 180 Hz., which falls between the (2,1) and (1,2) modes. It should be pointed out that, in the absence of internal damping and the PD, the time-averaged active intensity is zero.

Influence of Structural Damping. To examine the SI as a function of the structural damping, the SI vector map was computed with $C=0$, and $\eta=0.01$ and 0.1 at the resonance frequency of 280 Hz. and shown in Fig. 1a, together with the dynamic displacement field contour map shown in Fig. 1b. The latter clearly exhibits a slightly distorted (2,2) mode shape. The power flows from the point source at (0.15, 0.15 m) to all points in the plate. However, since the internal energy loss in the plate due to viscous type structural damping is proportional to the local kinetic energy density,

the power flows towards points of high velocities. Since there no other mechanisms of energy absorption, the total injected power from the point force is exclusively absorbed by the plate. Thus, increasing the structural damping coefficient from 0.01 to 0.1 resulted in a ten-fold increase in the input power as well as the maximum SI vector magnitude. One notes that in the absence of the point damper, a vortex-like flow is centered at the location (0.42, 0.20m.). This occurs when the $SI=0$, which must have both zero displacement and zero slopes in the x- and y- directions. It clearly falls on the nodal line of the (2,2) mode.

In the presence of the PD, part of the injected power is absorbed by the PD, and the remainder is absorbed internally by the structural damping in the plate. For example, for a low resistivity PD with $C=20$ N/sec, and $\eta=0, 0.01$ and 0.1 , the SI maps are shown in Figs 2(a,b,c), respectively. In all three cases, the displacement contour maps (not shown) exhibit the same (2,2) mode shape. However, it can be seen that when $\eta=0$, the energy flows from the source to the PD exclusively, and the input power is totally absorbed by the PD. When structural damping is low, i.e., $\eta=0.01$, part of the energy is absorbed by the entire plate(30%), and the remainder(70%) is absorbed by the PD. However, when the structural damping is high, e.g. $\eta=0.1$, then most of the power is absorbed by the plate before it reaches the PD, so that the plate absorbs 96% of the injected power, while only 4% of that power escapes through the PD.

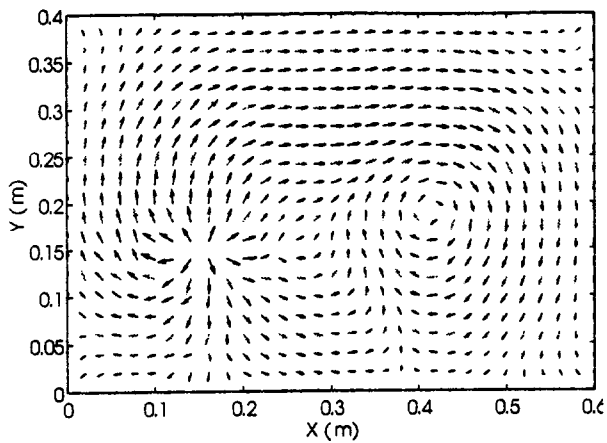
For off-resonance excitation at 180 Hz., the displacement field is a superposition of the two adjacent modes, namely the (1,2) and (2,1) modes, Fig 3b. When the PD is not present, $C=0$, power flows to regions of maximum kinetic energy density, Fig.3a. However, the vortex shifted to (0.3, 0.1m), again a point where the $SI=0$. With the PD present, the SI maps are similar to the resonance case. The injected power partition between the plate and the PD is similar to the resonance case, except that the input power at off-resonance is 13 dB lower than at resonance, as expected.

Influence of PD Absorptivity. To investigate the effect of the absorptivity on the power flow at resonance, the SI maps were plotted for values of C from 0 to 200 Nsec/m. The change of the SI maps is gradual so that only the extreme value $C=200$ Nsec/m is shown in Fig. 4a and 4b for $\eta=0.01$ and 0.1 , respectively. Comparing the SI maps in Fig.4a with 2b shows that when the structural damping is low, the flow to the PD is very pronounced, with the absorption by the PD increasing from 35 to 80% of the injected power. When the structural damping is high ($\eta=0.1$), the absorption by the PD increases from 4 to 20% of the injected power. However, the portion of the injected power left after absorption by the plate is actually small in either case. This means that the power flowing to the PD is small independent of its absorptivity. Similar comments can be made for the power flow at the off-resonance frequency of 180 Hz.

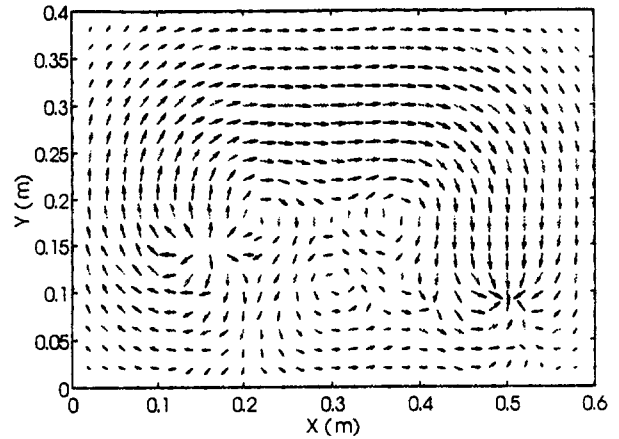
Conclusion.In conclusion, the power injected by a point source flows to a resistively connected structure if the plate structural damping is small. As the structural damping increases, the power flows less to the connected structure, as most of the power is absorbed by the plate, with little left to reach and be absorbed by the PD.

REFERENCES

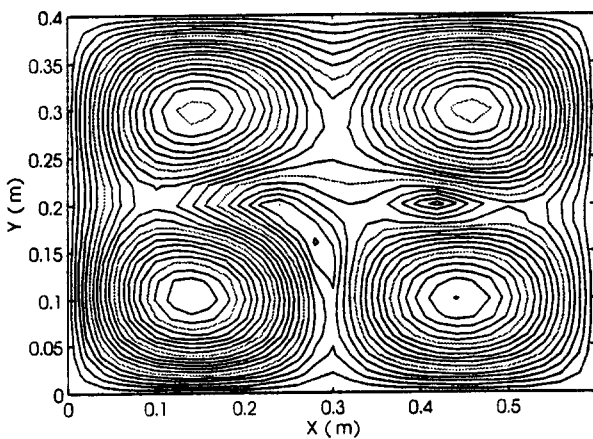
1. Proc. Third and Fourth Congresses on Structural Intensity and Vibrational Power Flow, Cetim, Senlis, France, August 27-29, 1990, and August 31-September 2, 1994, respectively.
2. Noiseux, D. U., "Measurement of Power Flow in Uniform Beams and Plates," J. Acoust. Soc. Am., 47(2), pp 238-247, (1970).
3. Pavic, G., "Measurement of Structure Borne Wave Intensity Part I: Formulation of the Methods," Journal of Sound and Vibration, 49, 221-230,1976.
4. Cuschieri, J. M., "Experimental Measurement of Structural Intensity on an Aircraft Fuselage," J. Noise Control Eng., 37(3), 97-107,1991.
5. Verheij, J. W., "Cross Spectral Density Methods for Measuring Structure Borne Power Flow on Beams and Pipes," Journal of Sound and Vibration, 70(1),133-139,(1980).
6. Hayek, S. I., M. J. Pechersky and B. C. Suen, " Measurement and Analysis of Near and Far Field Structural Intensity by Scanning Laser Vibrometry," Proc. International Congress on Intensity Techniques, Senlis, France, 27-29 April, 1990.
7. Williams, E.G., H. D. Dardy, R. G.Fink, " A Technique for Measurement of Structure-Borne Intensity in Plates." J. Acoust. Soc. Am., 78(6), 2061-2068, (1985).



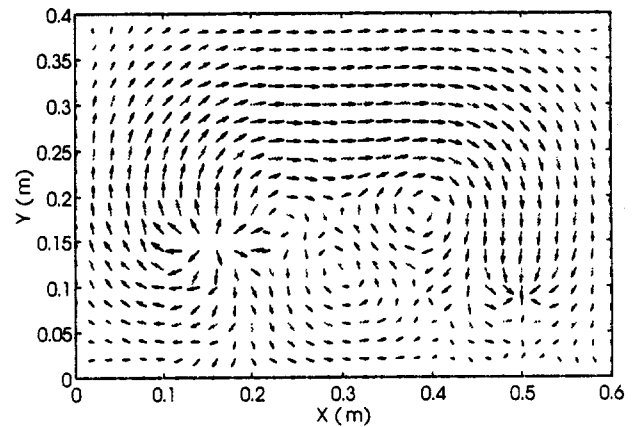
(a)



(a)

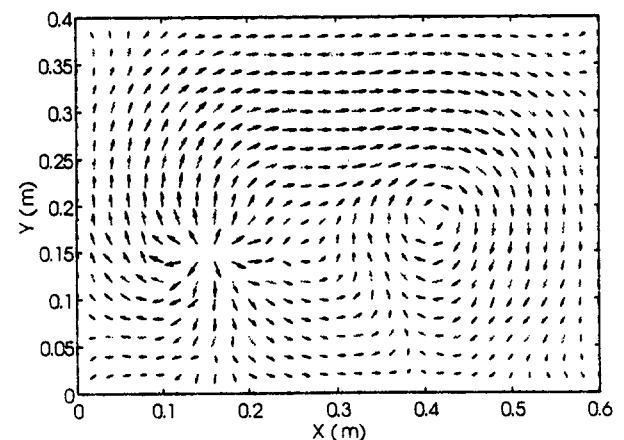


(b)



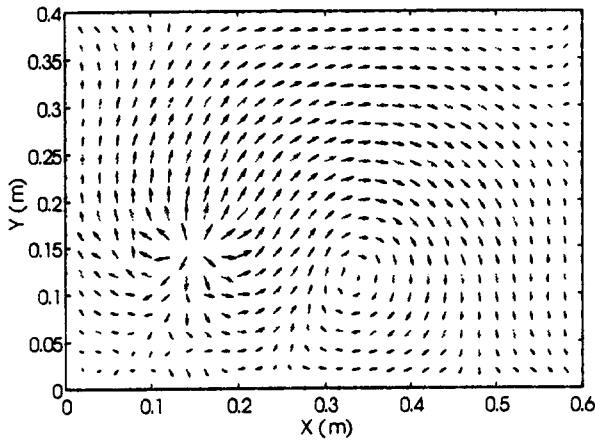
(b)

↑ Fig. 1 (a) Intensity normalized vector map (max. 8.96×10^{-3} N/sec, at damper 1.11×10^{-3} N/sec) (b) displacement contour (max. 1.87×10^{-6} m, at damper 1.22×10^{-6} m), 280 Hz, $C=0, \eta=0.1, \Pi_s=1.11 \times 10^{-3}$ Nm/sec

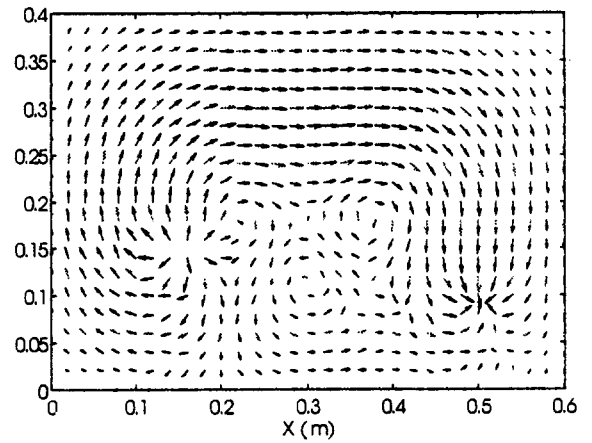


(c)

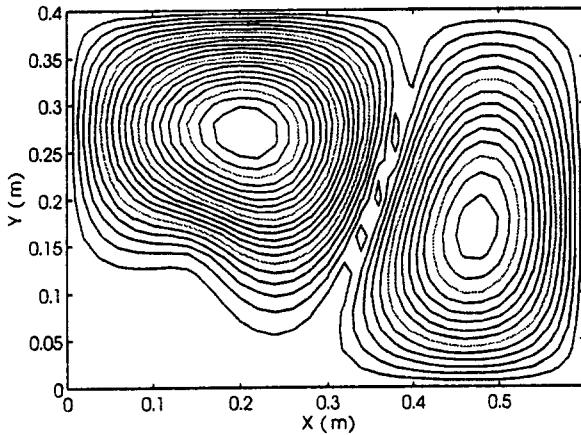
⇒ Fig. 2 Intensity normalized vector map 280 Hz, $C=20$ Nsec/m (a) $\eta=0$, max. 1.92×10^{-1} N/sec, at damper 5.82×10^{-2} N/sec, $\Pi_s=1.66 \times 10^{-2}$ Nm/sec, $\Pi_d=1.66 \times 10^{-2}$ Nm/sec (b) $\eta=0.01$, max. 5.25×10^{-2} N/sec, at damper 1.18×10^{-2} N/sec, $\Pi_s=6.01 \times 10^{-3}$ Nm/sec, $\Pi_d=2.21 \times 10^{-3}$ Nm/sec (c) $\eta=0.1$, max. 8.70×10^{-3} N/sec, at damper 1.08×10^{-3} N/sec, $\Pi_s=1.06 \times 10^{-3}$ Nm/sec, $\Pi_d=4.09 \times 10^{-5}$ Nm/sec



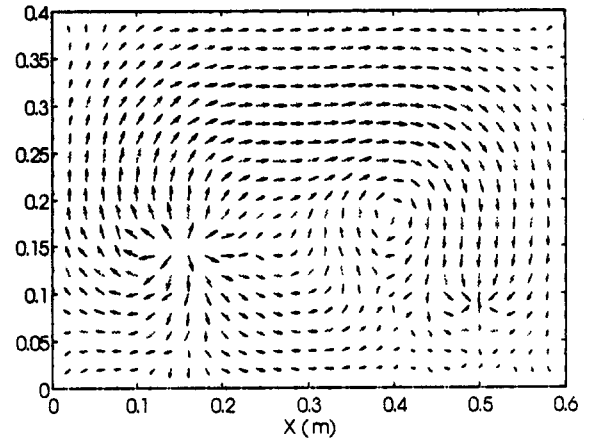
(a)



(a)



(b)



(b)

Fig. 3 (a) Intensity normalized vector map (max. 1.58×10^{-4} N/sec, at damper 8.89×10^{-6} N/sec) (b) Displacement contour (max. 1.79×10^{-6} m, at damper 9.63×10^{-7} m), 180Hz, $C=0, \eta=0.01, \Pi_s=2.00 \times 10^{-5}$ Nm/sec

Fig.4 Intensity normalized vector map 280Hz, $C=200$ Nsec/m
 (a) $\eta=0.01$, max. 1.43×10^{-2} N/sec, at damper 4.43×10^{-3} N/sec, $\Pi_s=1.48 \times 10^{-3}$ Nm/sec, $\Pi_d=1.21 \times 10^{-3}$ Nm/sec
 (b) $\eta=0.1$, max. 7.21×10^{-3} N/sec, at damper 9.30×10^{-4} N/sec, $\Pi_s=8.60 \times 10^{-4}$ Nm/sec, $\Pi_d=1.70 \times 10^{-4}$ Nm/sec